Available online at www.sciencedirect.com
SCIENCE DIRECT
Journal of Crystal Growth 288 (2006) 70–74
JOURNAL OF CRYSTAL GROWTH
www.elsevier.com/locate/jcrysgro

Preparation and characterization of nanocrystalline SnO_2 thin films by PECVD

Hui Huang*, O.K. Tan, Y.C. Lee, M.S. Tse

Microelectronics Center, School of Electrical and Electronic Engineering, Nanyang Technological University, 50 Nanyang Avenue, 639798 Singapore, Singapore

Available online 18 January 2006

Abstract

Nanocrystalline SnO_2 thin films were deposited by RF inductively coupled plasma enhanced chemical vapor deposition (PECVD) using dibutyltin diacetate as precursor. The effects of substrate–nozzle distance (D_{sn}), RF power and deposition time on the phase and morphologies of the SnO_2 thin films have been studied. The as-deposited SnO_2 thin films were well crystallized even without additional substrate heating and post-annealing. The grain size and film thickness decreased continuously with the increase of D_{sn} and RF power while increased with increasing deposition time. The deposition parameters showed notable effects on the microstructure of the SnO_2 thin films, thus it was possible to optimize the microstructure of the SnO_2 thin films by adjusting deposition parameters to achieve high-performance SnO_2-based thin film gas sensors.

PACS: 81.15.Gh; 81.07.Bc

Keywords: A3. Chemical vapor deposition processes; B1. Tin oxide

1. Introduction

SnO_2 is an important functional material and has been extensively investigated for gas sensors [1], electrocatalytic anodes [2] and optical-conductive coatings for solar cells [3]. Various processing routes, both physical and chemical deposition methods, have been utilized to prepare SnO_2 thin films, including pulsed laser deposition [4], radio frequency sputtering [5], sol–gel process [6], spray pyrolysis [7], electron beam evaporation [8] and PECVD [9]. Among them, PECVD was chosen as an ideal fabrication method for preparing nanostructured SnO_2 thin films basically due to its low deposition temperature.

For gas sensing application, the sensing mechanism of SnO_2 gas sensors is largely based on the surface reactions, where the concentration change of the surface adsorbed oxygen leading to conductivity change is associated with the detection of a specific gas in the environment. Recently, due to large surface-to-volume ratio and small grain size comparable to the depth of the surface space-charge layer, nanostructured SnO_2 thin films have stimulated great interests. Tan et al. [10] found that the nanocrystalline $x SnO_2$-$(1-x)\alpha Fe_2O_3$ with grain size down to 10 nm showed good sensitivity and selectivity to ethanol. Study on grain size effect in gas sensing by Yamazoe et al. [11,12] showed that the CO and H_2 gas sensitivity was greatly enhanced when the reduction of grain size to the range comparable to or less than two times depth of the surface space-charge layer. A linear relationship between SnO_2 sensor surface area and its sensitivity to H_2 was reported by Li and Kawi [13]. It was proven that microstructure optimization of sensor materials to achieve small grain size and large surface area was an effective way to obtain high gas sensitivity and selectivity for SnO_2-based gas sensors. Therefore, it is necessary to know how the preparation parameters affect on the microstructure of SnO_2 thin films before microstructure modifications are carried out.

*Corresponding author. Tel.: +65 6790 6387; fax: +65 6790 2631.
E-mail address: hhuang@ntu.edu.sg (H. Huang).

0022-0248/$ - see front matter © 2005 Published by Elsevier B.V.
doi:10.1016/j.jcrysgro.2005.12.031

In this paper, nanostructured SnO_2 thin films were prepared by PECVD and the effects of deposition parameters on the microstructure of SnO_2 thin films were studied. These preliminary results are helpful to optimize the microstructure of SnO_2 thin films to achieve high-performance SnO_2-based gas sensor.

2. Experimental procedure

The deposition system was a custom-designed PECVD system, and details of the system are shown in Ref. [14]. Inductively coupled plasma (ICP) was used as the plasma source and it was generated by a 13.56 MHz, 0.4–1.5 kW RF generator coupled on a copper tape circled around the cylindrical quartz deposition chamber. Dibutyltin diacetate (Aldrich, 98% purity), $(C_4H_9)_2Sn(OOCCH_3)_2$, was used as precursor. The precursor was soaked at 90 °C. Ar was used as the carrier gas at a flow rate of 100 and 100 sccm O_2 was used as the reaction gas. A 4″ SiO_2/Si wafer was used as the substrate and it was put in the downstream of the plasma for deposition. Neither additional substrate heating during deposition nor post-annealing was performed.

The phase of the films was studied by a Rigaku X-ray diffractometer (XRD) using Cu K_α radiation. The mean grain size was estimated by Scherrer's equation. A Leo 1550 field emission-type scanning electron microscopy (SEM) was used to observe the morphologies of the SnO_2 thin films. Thickness of the films was measured by a Filmetric F20 Thin-Film Measurement System and a J.A. Woollam VB-250 ellipsometer.

3. Results and discussions

3.1. Effect of substrate-nozzle distance

Substrate–nozzle distance (D_{sn}) was denoted as the distance between the substrate and the injection nozzle of vapor outlet. It should be indicated that the substrate was exactly located in the middle of the plasma for $D_{sn} = 12.5$ cm and the substrates position shifted to the downstream of the plasma for D_{sn} larger than 12.5 cm. Fig. 1 shows the XRD patterns of the SnO_2 thin films deposited at various D_{sn}. It indicated that the as-deposited SnO_2 thin films were well crystallized even without additional substrate heating. All diffraction peaks could be indexed by Cassiterite SnO_2 (PDF 41-1445). A shift of preferred orientation from the (1 0 1) plane to (1 1 0) plane was noted with the increase of D_{sn} from 12.5 to 24.5 cm. Fig. 2 shows the effect of D_{sn} on the thickness and mean grain size calculated by Scherrer's equation. As the D_{sn} increased from 12.5 to 24.5 cm, the grain size decreased from 17 to 5 nm while the thickness of the films also decreased dramatically.

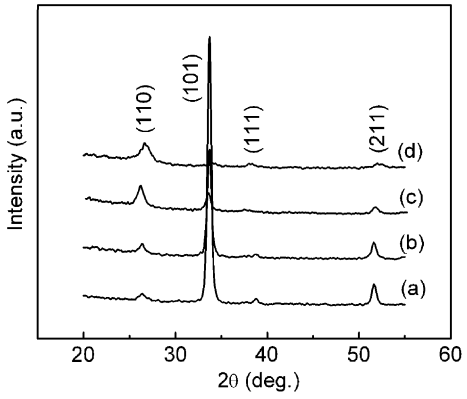

Fig. 1. XRD patterns of the SnO_2 thin films deposited at $D_{sn} = $ (a) 12.5 cm, (b) 16.5 cm, (c) 20.5 cm and (d) 24.5 cm.

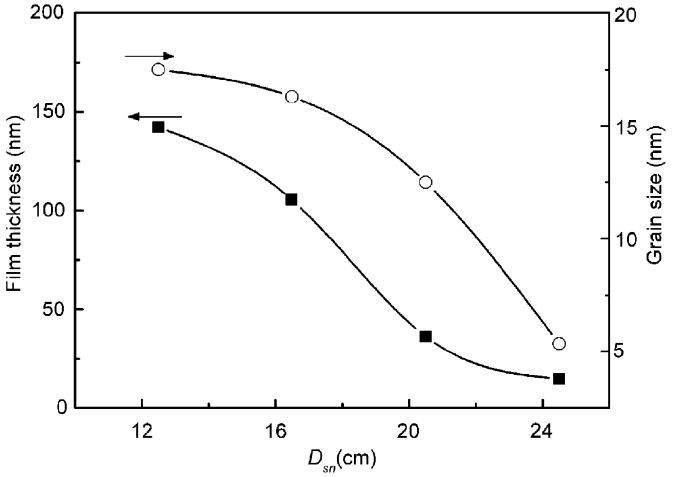

Fig. 2. Effect of D_{sn} on the thickness and grain size of the SnO_2 thin films.

Fig. 3 shows the SEM micrographs of the SnO_2 thin films deposited at $D_{sn} = $ (a) 12.5 cm, (b) 16.5 cm and (c) 20.5 cm. The SnO_2 thin film deposited in the middle of the plasma ($D_{sn} = 12.5$ cm) was porous and showed flower-like microstructure (Fig. 3a), which was possibly caused by the competition effect between deposition and plasma sputtering. The grains in the SnO_2 thin film deposited at 16.5 cm was regular in uniform size of 40 nm, and some tetragonal grains could be observed (Fig. 3b), which indicated that the films were well crystallized and developed. The SEM micrographs confirmed that the grain size of the films decreased with the increase of D_{sn}.

3.2. Effect of the RF power

Fig. 4 shows the XRD patterns of the SnO_2 thin films deposited at $D_{sn} = 20.5$ cm with RF power of (a) 400 W, (b) 800 W, (c) 1200 W and (d) 1500 W. Similar shift of preferred orientation from (1 0 1) plane to (1 1 0) plane as shown in Fig. 1 was observed with the increase of RF power from 400 to 1500 W. Fig. 5 shows the effect of RF power on the thickness and grain size of the SnO_2

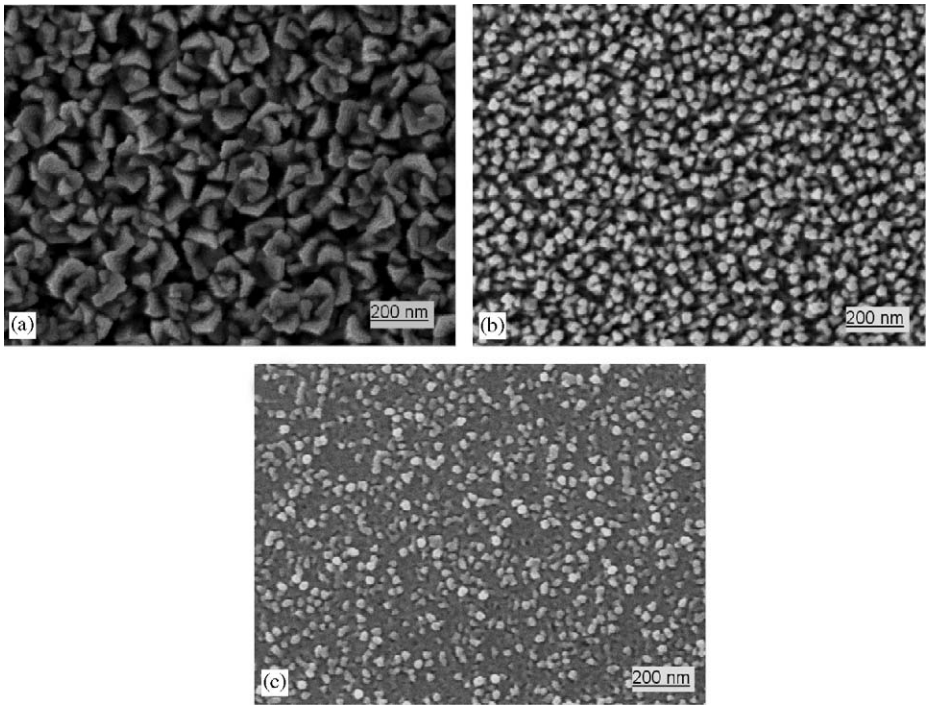

Fig. 3. SEM micrographs of the SnO_2 thin films deposited at D_{sn} = (a) 12.5 cm, (b) 16.5 cm and (c) 20.5 cm.

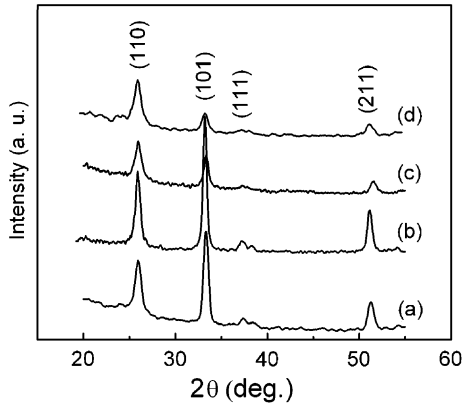

Fig. 4. XRD patterns of the SnO_2 thin films deposited at $D_{sn} = 20.5$ cm with RF power of (a) 400 W, (b) 800 W (c) 1200 W and (d) 1500 W.

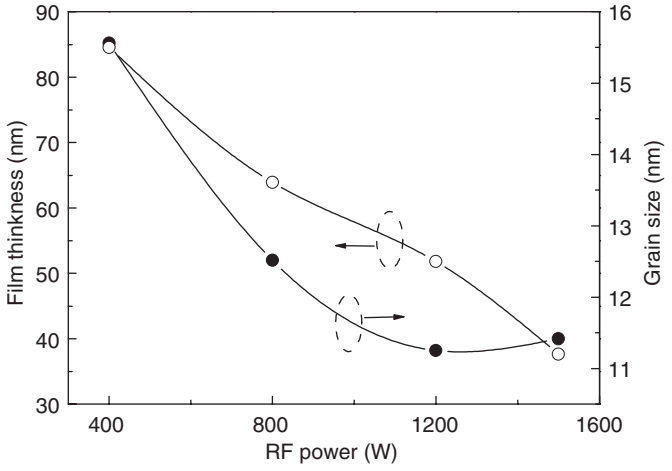

Fig. 5. Effect of RF power on the thickness and grain size of the SnO_2 thin films.

thin films. It showed that the grain size as well as the films thickness decreased with the increasing RF power. Higher RF power increases both electron density and energy, accelerating reactions of precursor in the plasma phase, which are both prerequisites for the formation of SnO_2 and SnO [15]. Thus, the concentration of the SnO_2 components is higher in the plasma, and results in a higher nuclei rate of SnO_2 in the plasma. It is known that higher nuclei rate consumes most of the precursor in a shorter time and results in a smaller grain size. However, as the clusters in the plasma with higher RF power are more active, they are likely to deposit on the chamber wall and cause precursor loss, which results in thinner films.

Fig. 6 shows the SEM micrographs of the SnO_2 thin films deposited at $D_{sn} = 20.5$ cm with RF power at (a) 400 W, (b) 800 W, (c) 1200 W and (d) 1500 W. The SnO_2 thin films deposited at 400 W were very smooth and dense, while the SnO_2 thin films deposited at higher RF power showed rough surface morphologies. The grain size of the SnO_2 thin films seemed to decrease with the increasing RF

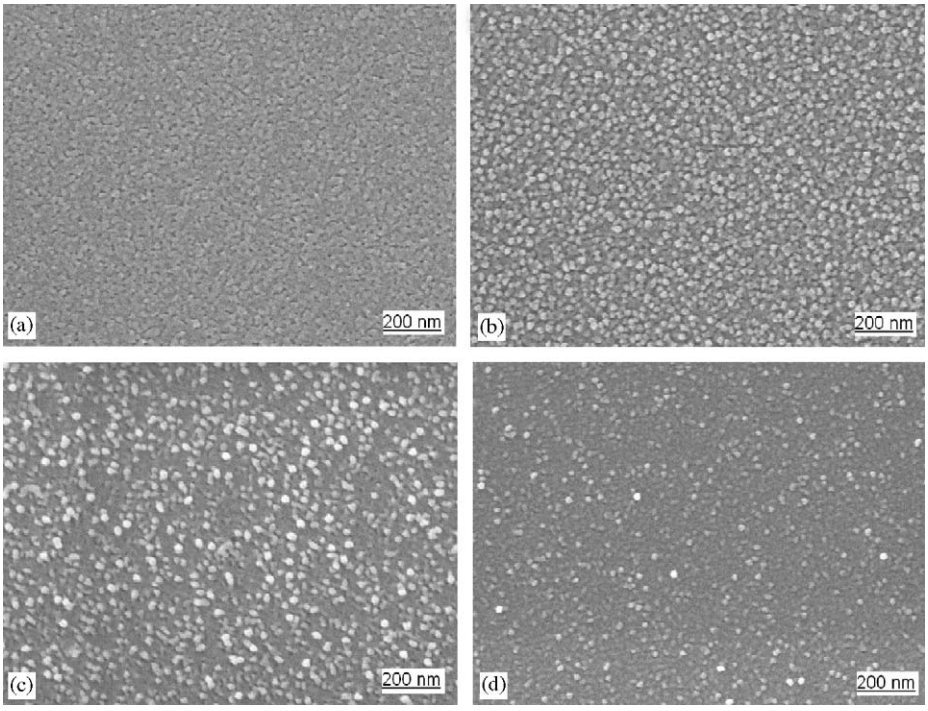

Fig. 6. SEM micrographs of the SnO_2 thin films deposited at $D_{sn} = 20.5$ cm with RF power of (a) 400 W, (b) 800 W, (c) 1200 W and (d) 1500 W.

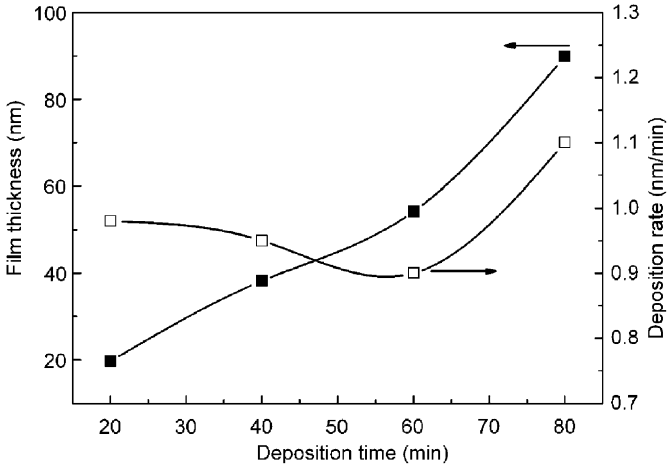

Fig. 7. Thickness and average deposition rate of the SnO_2 thin films deposited at increasing deposition time.

power, which was in accordance with the results obtained by Scherrer's equation (Fig. 5).

3.3. Effect of deposition time

Fig. 7 shows the thickness and average deposition rate of the SnO_2 thin films deposited at increasing deposition time. The thickness of the SnO_2 thin films increased with the increase of deposition time and the average deposition rate ranged from 0.9 to 1.1 nm/min.

Fig. 8 shows the SEM micrographs of the SnO_2 thin films deposited at 20.5 cm for (a) 20 min, (b) 40 min, (c) 60 min and (d) 80 min. The SnO_2 thin film deposited for 20 min was very dense and the grain size was 18 nm. With the deposition time increased to 80 min, the surface of the as-deposited films was rough and the grain size increased to 32 nm.

4. Conclusions

Nanocrystalline SnO_2 thin films were deposited on SiO_2/Si substrate by PECVD using dibutyltin diacetate as precursor. The as-deposited SnO_2 thin films were well crystallized even without additional substrate heating during deposition. The deposition parameters such as substrate distance, RF power and deposition time showed notable effects on the microstructure of the SnO_2 thin films, so the grain size and morphologies of the SnO_2 thin films can be optimized via the tuning of deposition parameters to achieve high-performance SnO_2-based gas sensors.

Acknowledgments

This work is sponsored by the A*STAR of Singapore (No. 0221010022).

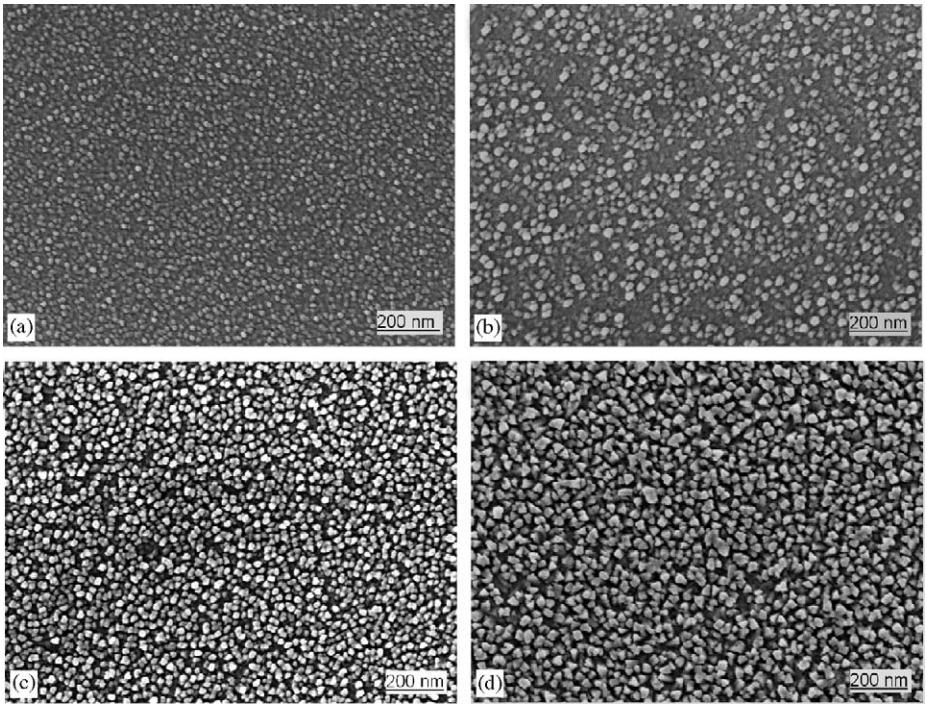

Fig. 8. SEM micrographs of the SnO_2 thin films deposited at 20.5 cm for (a) 20 min, (b) 40 min, (c) 60 min and (d) 80 min.

References

[1] P. Ménini, F. Parret, M. Guerrero, K. Soulantica, L. Erades, A. Maisonnat, B. Chaudret, Sensors Actuators B: Chem. 103 (2004) 111.
[2] P. Duverneuil, F. Maury, N. Pebere, F. Senocq, H. Vergnes, Surf. Coat. Technol. 151–152 (2002) 9.
[3] B.V. Bergeron, A. Marton, G. Oskam, G.J. Meyer, J. Phys. Chem. B 109 (2005) 937.
[4] M.A. El Khakani, R. Dolbec, A.M. Serventi, M.C. Horrillo, M. Trudeau, R.G. Saint-Jacques, D.G. Rickerby, I. Sayago, Sensors Actuators B: Chem. 77 (2001) 383.
[5] A. Karthigeyan, R.P. Gupta, M. Burgmair, S.K. Sharma, I. Eisele, Sensors Actuators B: Chem. 87 (2002) 321.
[6] C. Cobianu, C. Savaniu, P. Siciliano, S. Capone, M. Utriainen, L. Niinisto, Sensors Actuators B: Chem. 77 (2001) 496.
[7] G. Korotcenkov, V. Brinzari, J. Schwank, A. Cerneavschi, Mater. Sci. Eng. C 19 (2002) 73.
[8] Y.W. Mo, Y. Okawa, T. Nakai, M. Tajima, K. Natukawa, Thin Solid Films 416 (2002) 248.
[9] F. Hellegouarc'h, F. Arefi-Khonsari, R. Planadel, J. Amouroux Sensors Actuators B: Chem. 73 (2001) 27.
[10] O.K. Tan, W. Zhu, Q. Yan, L.B. Kong, Sensors Actuators B: Chem. 65 (2000) 361.
[11] N. Yamazoe, Sensors Actuators B: Chem. 5 (1991) 7.
[12] C. Xu, J. Tamaki, N. Miura, N. Yamazoe, Sensors Actuators B: Chem. 3 (1991) 147.
[13] G.J. Li, S. Kawi, Mater. Lett. 34 (1998) 99.
[14] Y.C. Lee, O.K. Tan, M.S. Tse, A. Srivastava, Ceram. Int. 30 (2004) 1869.
[15] J.J. Robbins, R.T. Alexander, W. Xiao, T.L. Vincent, C.A. Wolden, Thin Solid Films 406 (2002) 145.